Upper-Level Eddy Angular Momentum Fluxes and Tropical Cyclone Intensity Change

MARK DEMARIA,* JONG-JIN BAIK,**,† AND JOHN KAPLAN*

*Hurricane Research Division, AOML/NOAA, Miami, Florida
**Severe Storms Branch, NASA/Goddard Space Flight Center, Greenbelt, Maryland

(Manuscript received 24 October 1991, in final form 1 July 1992)

ABSTRACT

The eddy flux convergence of relative angular momentum (EFC) at 200 mb was calculated for the named tropical cyclones during the 1989–1991 Atlantic hurricane seasons (371 synoptic times). A period of enhanced EFC within 1500 km of the storm center occurred about every 5 days due to the interaction with upper-level troughs in the midlatitude westerlies or upper-level, cold lows in low latitudes. Twenty-six of the 32 storms had at least one period of enhanced EFC.

In about one-third of the cases, the storm intensified just after the period of enhanced EFC. In most of the cases in which the storm did not intensify the vertical shear increased, the storm moved over cold water, or the storm became extratropical just after the period of enhanced EFC. A statistically significant relationship (at the 95% level) was found between the EFC within 600 km of the storm center and the intensity change during the next 48 h. However, this relationship could only be determined using a multiple regression technique that also accounted for the effects of vertical shear and sea surface temperature variations.

The EFC was also examined for the ten storms from the 1989–1991 sample that had the largest intensification rates. Six of the ten periods of rapid intensification were associated with enhanced EFC. In the remaining four cases the storms were intensifying rapidly in a low shear environment without any obvious interaction with upper-level troughs.

1. Introduction

Theoretical and observational studies (e.g., Emanuel 1988; Merrill 1988) indicate that the maximum intensity that a tropical cyclone can attain is limited by the sea surface temperature (SST). However, only a small percentage of storms actually reach this upper bound. One explanation for this lack of intensification is the effect of vertical wind shear in the storm environment (e.g., Gray 1968). Another explanation is that the storm circulation reduces SST through mixing and upwelling (e.g., Khain and Ginis 1991).

There is also evidence that interactions between a tropical cyclone and its environment can lead to intensification of the storm. Numerous studies have shown that rapid intensification often occurs when there is an upper-level trough several hundred kilometers to the west and poleward of a storm (e.g., Sadler 1976). Pfeffer (1958) suggested that the interaction between a tropical cyclone and its environment can be quantified by calculating momentum transports due to azimuthal eddies in a storm-centered coordinate system. McBride (1981) showed that in a composite of intensifying storms there was a large inward eddy flux of cyclonic angular momentum in the outflow layer. Two-dimensional modeling studies with specified upper-level momentum fluxes (Pfeffer and Challa 1981) and three-dimensional simulations with initial conditions from composite developing and nondeveloping tropical disturbances (Challa and Pfeffer 1990) indicate that upper-level eddy angular momentum fluxes (EFCs) can lead to tropical cyclone intensification. In a case study of Hurricane Elena (1985), Molinari and Vollaro (1989, 1990) showed that upper-level eddy fluxes were important for the intensification of the storm. In case studies of tropical cyclones Irma and Jason in the Australian region, Davidson et al. (1990) suggested that the upper-level eddy momentum fluxes played a role in the genesis of these two storms.

In contrast to the above results, Merrill (1988) showed that no clear relationship existed between intensity change and eddy momentum fluxes in a 5-year composite of Atlantic hurricanes. Large eddy fluxes are often associated with the interaction between a storm and an upper-level trough. Merrill (1988) speculated that the positive influences of the eddy fluxes might be offset by the negative influences of increased vertical wind shear associated with the trough.

Most of the observational studies of eddy momentum fluxes have used composited data or considered

† Universities Space Research Association Research Associate.

Corresponding author address: Dr. Mark DeMaria, United States Department of Commerce, NOAA/AOML, 4301 Rickenbacker Causeway, Miami, FL 33149.

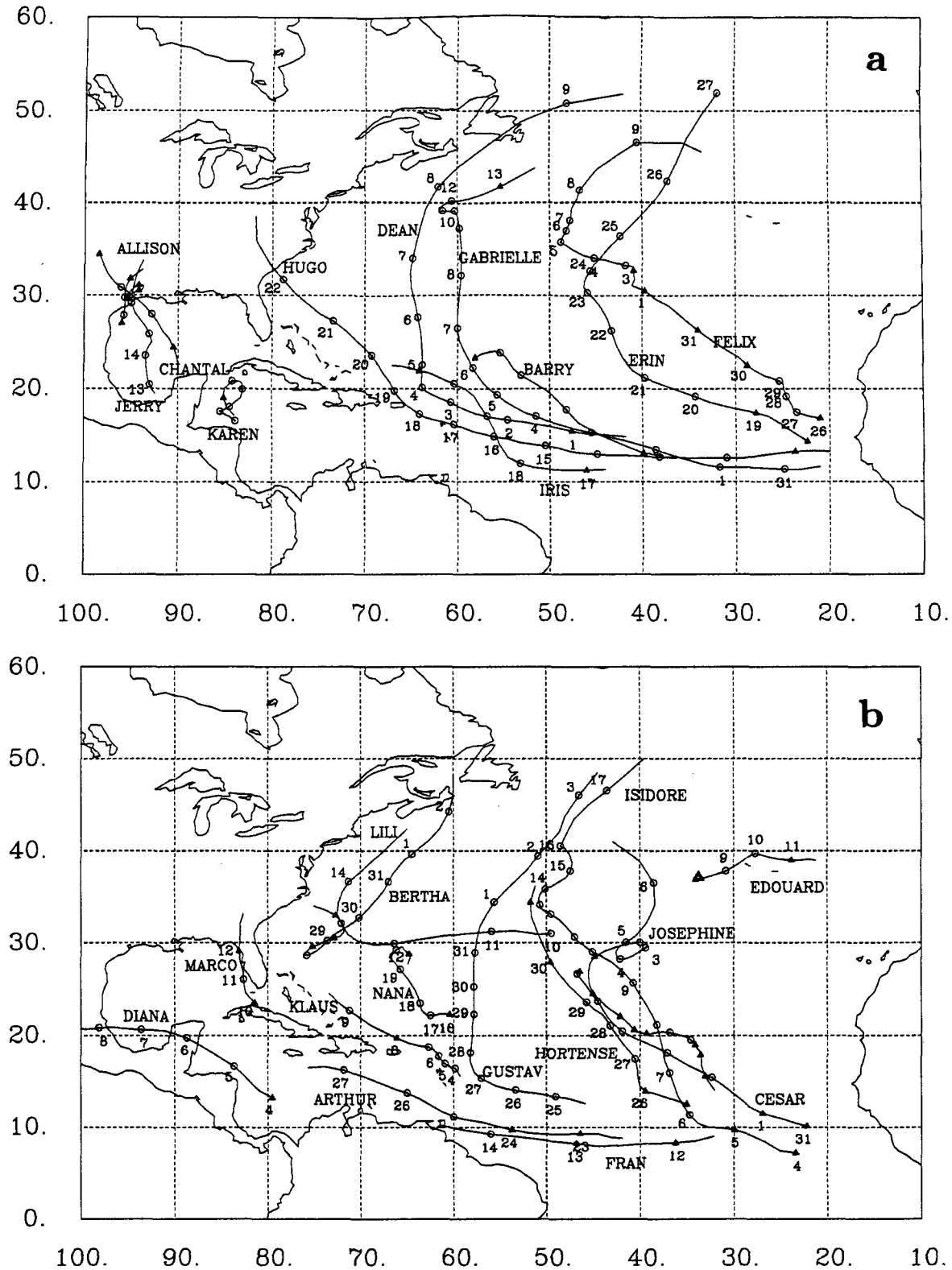

FIG. 1. Tracks of the Atlantic tropical cyclones during the (a) 1989, (b) 1990, and (c) 1991 hurricane seasons. The 0000 UTC positions are plotted as a circle (triangle) when the storm intensity was greater (less) than tropical storm strength. The day of the month is plotted next to the storm positions when possible.

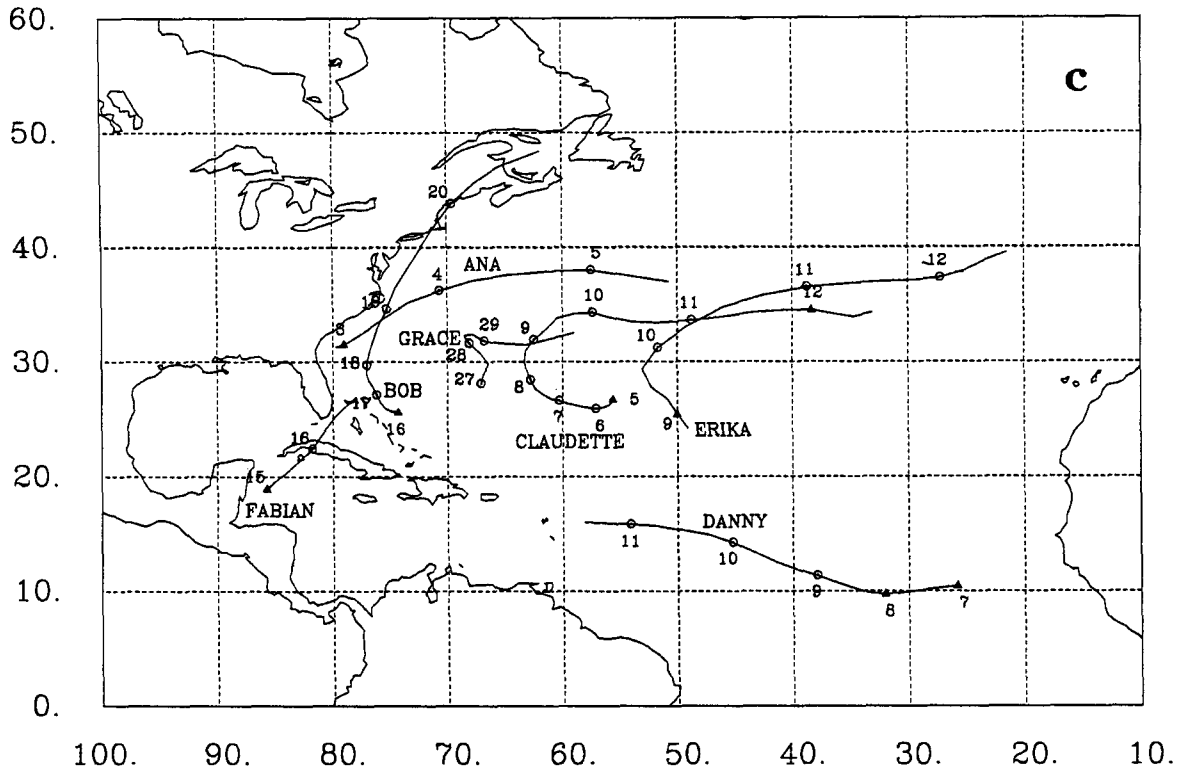

FIG. 1. (*Continued*)

case studies of a small number of storms. In this study, the effects of upper-level eddy momentum fluxes on tropical cyclone intensity change were examined for all of the named storms during the 1989–1991 Atlantic hurricane seasons. Vertical wind shear and SST were also considered to help separate positive and negative influences on intensity change.

For each storm, 200-mb wind analyses generated by the spline-fitting technique described by Lord and Franklin (1987) at 12-h intervals (0000 and 1200 UTC) were used to calculate the eddy angular momentum fluxes. This 3-year "climatology" was used to determine the magnitudes of the eddy fluxes during interactions with synoptic-scale weather systems and to estimate the frequency of the interactions. Simple regression techniques were used to determine if statistically significant relationships exist between upper-level eddy fluxes and tropical cyclone intensity change. The data and analysis method are described in section 2. In section 3, case studies of storms with strong momentum fluxes are presented, and the statistical regression is described in section 4. In section 5, the environmental interactions for the rapidly intensifying cases are examined.

2. Data and analysis method

Since 1989, synoptic data for Atlantic tropical cyclone cases have been collected and analyzed in near-real time to test an experimental track prediction model (DeMaria et al. 1992). Although the prediction model is barotropic, the data were analyzed at 850, 700, 500, and 200 mb and then vertically averaged to obtain the model initial condition. These analyses have been used in the current study to determine the 200-mb eddy angular momentum flux and the 200–850-mb vertical wind shear for the named storms during the 1989–1991 hurricane seasons.

The data used in the spline analyses included rawinsondes, satellite cloud-track winds, and aircraft observations from both U.S. Air Force reconnaissance and NOAA research missions. Aircraft observations were available in about half of the cases and were never available above 350 mb. The primary data sources over the open oceans were the satellite cloud-track winds. These winds were usually assigned to the 200- or 850-mb level. For this reason, the momentum fluxes were calculated only at 200 mb, and the vertical shear was evaluated using the 850- and 200-mb analyses.

Horizontal wind components (u and v) were analyzed by fitting cubic B-splines with a derivative constraint, where the constraint acts as a low-pass spatial filter (Ooyama 1987). The data were analyzed over a 40° lat by 40° long area (30° by 30° for the 1990 cases) centered on the storm. A National Meteorological Center (NMC) analysis was used as a low-weighted background field, and the derivative constraint was chosen so that the half-amplitude wavelength of the spatial filter was 4° latitude. In regions of poor data coverage the spline analysis reproduced the NMC analysis. In regions of relatively good coverage smaller horizontal scales were included in the spline analyses than in the NMC analyses. These analyses were produced every 12 h (0000 and 1200 UTC), and the horizontal winds were archived on a 1° lat by 1° long grid. Further details on the spline analysis technique can be found in Lord and Franklin (1987).

In this study, the storm intensity was measured by maximum surface winds that were obtained from the "best track" data (Jarvinen et al. 1984) archived by the National Hurricane Center (NHC). Because the maximum winds are forecast and archived in knots rounded to the nearest 5, these units have been used here. Figure 1 shows the tracks, and Table 1 lists the maximum intensity of the storms considered. There are 32 named storms in the sample, 18 of which reached hurricane intensity (maximum winds > 64 kt). All of the storms in 1989 formed from tropical waves. In 1990, several storms formed from extratropical systems (Bertha, Edouard, Lili, Marco, and Nana). In 1991, only two storms formed from tropical waves (Danny and Erika).

Most quantitative studies of the interaction of tropical cyclones and their environments have used the balanced vortex model (Eliassen 1952). This model describes the evolution of a two-dimensional vortex (a function of radius and height), where the azimuthally averaged tangential wind is in gradient balance with the azimuthally averaged pressure gradient. A diagnostic equation can be derived for the streamfunction that determines the secondary circulation (radial and vertical velocities). This secondary circulation maintains gradient balance in the presence of heat and momentum sources.

Following Molinari and Vollaro (1990), the secondary circulation equation in a storm-relative coordinate system can be written as

$$L\psi = r\partial/\partial p[(2\bar{V}_L/r + f)M] + (r\pi R/P)\partial H/\partial r, \quad (1)$$

where

$$M = -r^{-2}\partial/\partial r(r^2\overline{U'_L V'_L}) - \partial/\partial P(\overline{\omega' V'_L}) - \overline{f' U'}, \quad (2)$$

and

$$H = -r^{-1}\partial/\partial r(r\overline{\theta' U'_L}) - \partial/\partial P(\overline{\theta'\omega'}). \quad (3)$$

In (1)–(3), r is the radius, P the pressure, U the radial wind, V the tangential wind, ω the pressure vertical velocity, θ the potential temperature, ψ the streamfunction for the secondary circulation, π a function of pressure, f the Coriolis parameter, R the gas constant for dry air, and L represents a second-order linear elliptic operator. The overbar in (1)–(3) denotes an azimuthal average, the prime represents a deviation from the azimuthal average, and the subscript L on U or V indicates that these quantities are evaluated in a Lagrangian coordinate system (moving with the storm). The effects of friction and diabatic heating have been neglected in (1)–(3), even though these effects are large near the storm center. These processes are not included since the concern here is with interactions in the storm environment away from the inner-core region of the storm.

With wind analyses at only a few levels, it is not possible to evaluate all of the forcing terms in (1) or to solve this equation for the streamfunction. However, there is some evidence that the dominant contribution to the forcing is from the first term on the right side of (2), evaluated in the outflow layer of the storm.

The M and H terms in (1) represent eddy momentum and heat fluxes. Molinari and Vollaro (1990) showed that for the interaction of Hurricane Elena with

TABLE 1. Named Atlantic tropical cyclones during 1989–1991.

Storm	Maximum wind (kt)	Dates (mo/d)	Year
1 Allison	45	6/24–6/27	1989
2 Barry	45	7/09–7/14	1989
3 Chantal	70	7/30–8/03	1989
4 Dean	90	7/31–8/08	1989
5 Erin	90	8/18–8/27	1989
6 Felix	75	8/26–9/09	1989
7 Gabrielle	125	8/30–9/13	1989
8 Hugo	140	9/10–9/22	1989
9 Iris	60	9/16–9/21	1989
10 Jerry	75	10/12–10/16	1989
11 Karen	50	11/24–12/04	1989
12 Arthur	60	7/22–7/27	1990
13 Bertha	70	7/24–8/02	1990
14 Cesar	45	7/31–8/07	1990
15 Diana	85	8/04–8/09	1990
16 Edouard	40	8/02–8/11	1990
17 Fran	35	8/11–8/14	1990
18 Gustav	105	8/24–9/03	1990
19 Hortense	55	8/25–8/31	1990
20 Isidore	85	9/04–9/17	1990
21 Josephine	75	9/21–10/06	1990
22 Klaus	70	10/03–10/09	1990
23 Lili	65	10/06–10/14	1990
24 Marco	55	10/09–10/12	1990
25 Nana	75	10/16–10/21	1990
26 Ana	45	7/03–7/05	1991
27 Bob	100	8/16–8/21	1991
28 Claudette	115	9/04–9/14	1991
29 Danny	45	9/07–9/11	1991
30 Erika	50	9/08–9/12	1991
31 Fabian	40	10/15–10/17	1991
32 Grace	85	10/25–11/02	1991

a midlatitude trough, the secondary circulation response from the eddy heat fluxes was only about 20% of the response due to momentum fluxes. In addition, the secondary circulation due to the heat fluxes was in the same direction as that due to momentum fluxes. Pfeffer and Challa (1991) also evaluated the secondary circulation due to heat and momentum fluxes from a data composite of prehurricane depressions. Their results also showed that the response to the heat fluxes was in the same sense as that due to momentum fluxes, but was weaker within several hundred kilometers of the vortex center. Therefore, neglecting the effects of eddy heat fluxes is probably not a severe approximation.

The eddy momentum flux M in (2) has contributions from three terms. The first term on the right side of (2) represents the eddy flux convergence of relative angular momentum. Assuming scales valid for the synoptic environment, the second term on the right side of (2) is an order of magnitude smaller than the first term on the right side and is neglected. The third term on the right side of (2) represents the effect of the meridional flow (north–south) on the vortex. For a constant horizontal flow on a beta plane, it can be shown that the third term is given by $-1/2\beta vr$, where v is the northward component of the wind, and β is the northward gradient of the Coriolis parameter. Thus, the third term should be small near the vortex center (because of the dependence on r). Calculations using the 200-mb spline analyses showed that the magnitude of the third term on the right in (2) was about a factor of 5 less than the magnitude of the first term, within a few hundred kilometers of the storm center. Therefore, only the first term on the right in (2) is considered in this study.

Although the operator L in (1) is linear, it has coefficients that depend on the structure of the balanced vortex. Holland and Merrill (1984) determined the streamfunction using (1) with idealized momentum forcing. Their results showed that the response to forcing in the lower troposphere cannot penetrate to the vortex center. This is because the inertial stability due to the rapid rotation of the balanced vortex produces strong resistance to horizontal motion. However, in the upper troposphere where the inertial stability is small, the response to external forcing can penetrate to the vortex center. This result suggests that upper-level momentum forcing is much more likely to affect the intensity of a storm than low-level forcing.

TABLE 2. Mean and standard deviation of EFC in each radial band.

Radial band (km × 100)	Mean (m s^{-1} d^{-1})	Standard deviation
1–3	1.3	7.7
4–6	3.9	9.1
7–9	4.7	9.7
10–12	4.1	8.7
13–15	3.2	8.4

TABLE 3. Percentage distribution of average EFC for each radial band.

EFC (m s^{-1} d^{-1})	Radial band (km × 100)				
	1–3	4–6	7–9	10–12	13–15
< −20	1	0	0	1	1
−20 to −10	4	6	5	3	3
−10 to 0	43	31	28	29	34
0 to 10	43	45	46	50	48
10 to 20	7	13	14	12	11
> 20	2	5	7	5	3

The above discussion suggests that some information about the interaction of a tropical cyclone and its environment can be determined by consideration of the first term on the right side of (2) in the outflow layer of the storm. This term is referred to as EFC and the sign is such that when EFC is positive, the eddy fluxes are acting to make the upper-level flow more cyclonic (or less anticyclonic). The 200-mb spline analyses were used to evaluate EFC in a storm-centered cylindrical coordinate system at 100-km radial intervals from r = 100 to r = 1500 km. The storm motion was subtracted from the horizontal wind components to give the necessary storm-relative winds. To allow easy comparison with previous studies, EFC was calculated in units of m s^{-1} d^{-1}.

The secondary circulation equation (1) contains the vertical derivative of M (approximated by EFC in this study). If EFC increases with height up to the outflow layer, then the secondary circulation in the balanced model will be conducive to tropical cyclone intensification (upward motion through a deep layer). The EFC in the case study of Molinari and Vollaro (1990) and in the data composites presented by Challa and Pfeffer (1990) increased with height and reached a maximum at about 200 mb. This increase might be expected since large values of EFC are often associated with upper-level cold-core troughs with amplitudes that increase with height in the troposphere. Therefore, even though the EFC is only measured at a single level in

TABLE 4. Summary of enhanced EFC events.

Magnitude of event	Storm response	Environmental factors	Number of cases	Percent of cases
Moderate	Intensify	—	7	18
Moderate	Weaken	Decreasing SST	2	5
Moderate	Weaken	Increasing shear	8	21
Moderate	Weaken	Extratropical	1	3
Strong	Intensify	—	6	15
Strong	Weaken	Decreasing SST	3	8
Strong	Weaken	Increasing shear	2	5
Strong	Weaken	Extratropical	9	23
Strong	Weaken	Landfall	1	3

the current study, it is reasonable to assume that the magnitude of EFC increases with height up to 200 mb so that positive EFC should be correlated with intensification.

An important issue to address is the accuracy with which EFC can be calculated using the spline analyses. For example, the lack of a relationship between EFC and intensity change could result from inaccurate EFC values and not imply anything about environmental interactions. The spline analyses used to calculate EFC refine the NMC analyses used as a background field. Molinari et al. (1992) carefully evaluated analyses generated by a four-dimensional data assimilation system (similar to the NMC background fields). Their results show that in the vicinity of even a small number of rawinsondes (such as in the Gulf of Mexico or the Caribbean), the analyses are useful for studies of the tropical cyclone environment. Using a special set of manually produced satellite cloud track winds for verification, Molinari et al. (1992) showed that at 200 mb, estimates of EFC are accurate to within about 50%. As will be shown in the next section, EFC at 200 mb increases by a factor of 3 or more as a tropical cyclone interacts with an upper-level trough. Therefore, even with an error of 50%, it should be possible to distinguish periods of interaction from periods of noninteraction.

The discussion of (1)–(3) suggests that periods of enhanced EFC represent a positive interaction between a storm and its environment. The negative influence of the environment is quantified by the vertical shear of the horizontal wind. If the vertical shear is too large, temperature and moisture anomalies associated with the inner core of the storm are advected away from the low-level circulation, and development is inhibited (e.g., Anthes 1982). The vertical wind shear in the vicinity of the storm was calculated from the 850- and 200-mb wind analyses. The horizontal wind components within 600 km of the storm center were averaged to determine the mean environmental wind vector at each level. The vertical shear is the magnitude of the difference between the mean wind vectors at 850 and 200 mb.

As described in the Introduction, the maximum intensity of a storm is limited by the SST. Merrill (1988) determined an empirical relationship between the maximum storm intensity (VSST) and SST, given by

$$\text{VSST} = 74 \exp[0.2(\text{SST} - 25.0)], \qquad (4)$$

where VSST is in knots and SST is in degrees Celsius. The above relationship was developed from the observed maximum intensity of Atlantic tropical cyclones from several hurricane seasons, stratified by climatological SST. It is useful for estimating the additional intensification that might be expected for a given storm.

The SST values in (4) were determined from the climatology described by Levitus (1982). Digitized values of SST on a 1° lat by 1° long grid were available for each month. These values were linearly interpolated in space and time to the position and day of the storm.

3. Case study results

The EFC as a function of radius and time was calculated for all of the named tropical cyclones during the 1989–1991 hurricane seasons, using the method described in section 2. Analyses were available at 371 synoptic times and included the depression, tropical storm, and hurricane stages of each tropical system. EFCs on the 100-km radial grid were averaged over five radial bands (100–300, 400–600, 700–900, 1000–1200, and 1300–1500 km) to give a general idea of the storm to storm variation in the eddy fluxes.

It would be extremely useful if there was a complete theory that could predict the amount of intensification that might be expected for a given magnitude and structure of EFC. However, even the relatively large values of EFC reported by Molinari and Vollaro (1990) do not produce a secondary circulation strong enough to explain the observed storm intensification rates. In all of the studies on the effect of EFC, it is assumed that the induced secondary circulation interacts with

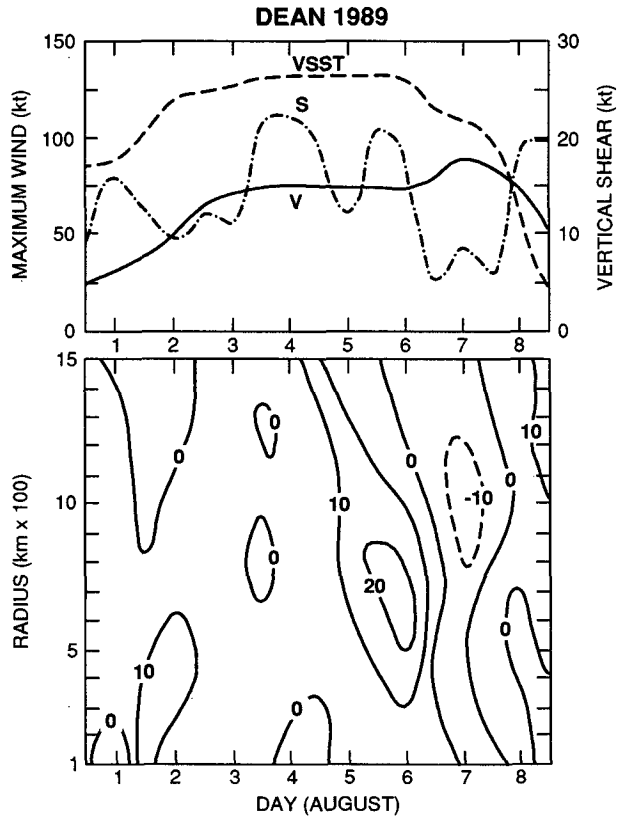

FIG. 2. The time evolution of the maximum wind (V), maximum expected wind (VSST) from Eq. (4), and vertical wind shear (S), (upper panel) and the eddy angular momentum flux convergence in the units of m s^{-1} d^{-1} as a function of radius and time (lower panel) for Hurricane Dean (1989).

the convection near the storm center. It is the enhancement of the convection that is assumed to cause the intensity change.

In a study of tropical cyclone development, Montgomery and Farrell (1993) included the effects of convection in two- and three-dimensional balanced models by assuming that rising air is saturated along angular momentum surfaces. The positive interaction between an upper-level trough and a low-level cyclonic circulation was greatly enhanced when moist processes were included. In principle, a similar assumption could be made in the balanced vortex model. One of the coefficients of the operator L in (1) is the static stability. If the dry static stability were replaced by the static stability associated with saturated ascent, the response to the upper-level EFC would probably be enhanced. In this case, the secondary circulation might be strong enough to explain the observed intensification rates. However, this calculation would require more detailed analyses of the inner core of the storm and greater vertical resolution than is available in our analyses.

Without direct theoretical guidance, the statistical distribution of the observed EFC was used to identify periods of enhanced EFC. Table 2 shows the average and standard deviation of EFC in each radial band. The average EFC is positive, with a maximum of about 5 m s^{-1} d^{-1} in the 700–900-km band. The mean positive value of EFC is consistent with the results of McBride (1981), which showed that the azimuthal eddies import cyclonic angular momentum in composites of Atlantic tropical cloud clusters, depressions, and tropical cyclones. The positive average value of EFC is probably due to the asymmetric nature of the outflow that is associated with each system. In this study, the primary interest is in the cases where EFC exceeds the mean value due to interactions with other weather systems.

Table 2 shows that EFC values one standard deviation greater than the mean range between 9 m s^{-1} d^{-1} for the 100–300-km radial band to about 14 m s^{-1} d^{-1} for the 700–900-km radial band. Based upon these results, we considered an EFC value of 10 m s^{-1} d^{-1} to

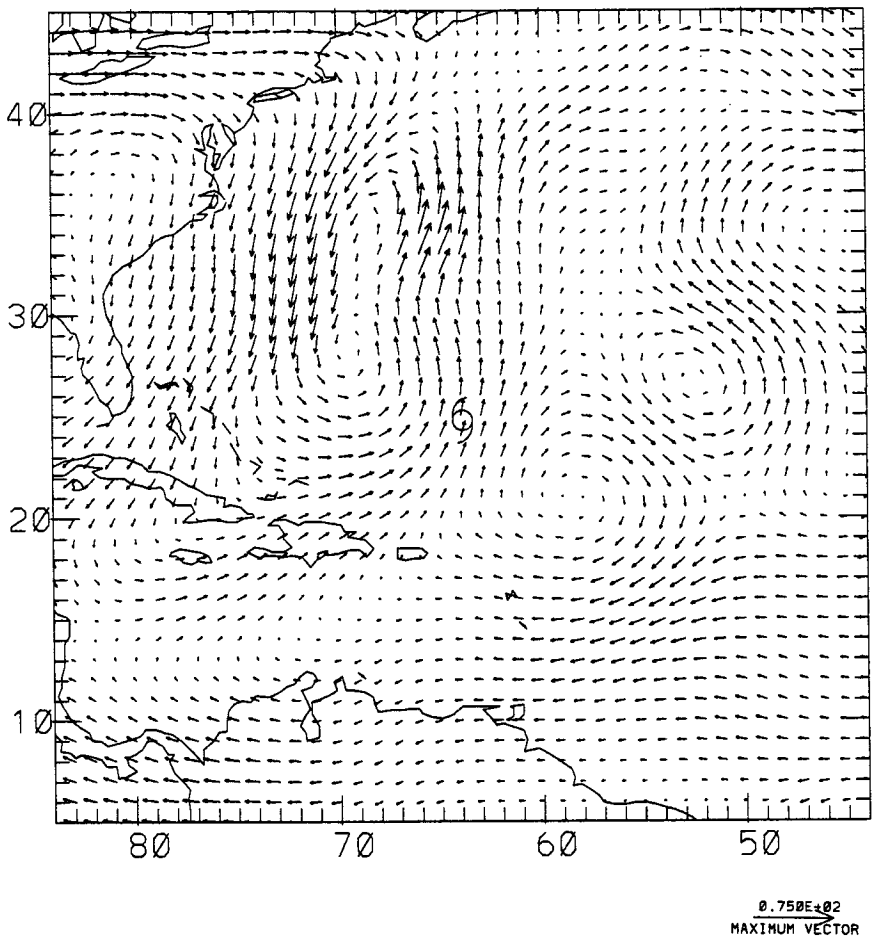

FIG. 3. The horizontal wind field at 200 mb for Hurricane Dean at 1200 UTC 5 August 1989. The storm center is indicated by the tropical cyclone symbol. Maximum wind vector: 75 m s^{-1}.

indicate a period of significant environmental interaction.

Table 3 shows the distribution of EFC in each radial band. EFC exceeded 10 m s^{-1} d^{-1} in about 9% of the cases for the 100–300-km radial band and in about 21% of the cases for the 700–900-km radial band. EFC also exceeded 20 m s^{-1} d^{-1} in some cases. In the following discussion, cases with EFC values between 10 and 20 m s^{-1} d^{-1} are referred to as moderate events, while cases having EFC values > 20 m s^{-1} d^{-1} are termed strong events.

The distribution of EFC in Table 3 is consistent with the values of EFC in other studies. In the case study by Molinari and Vollaro (1990), EFC values of up to 27 m s^{-1} d^{-1} were associated with the interaction of Hurricane Elena and a midlatitude trough. Davidson et al. (1990) showed that EFC values of about 8 m s^{-1} d^{-1} were associated with the interaction of a developing tropical cyclone and a tropical upper-tropospheric trough (TUTT). Challa and Pfeffer (1990) found EFC values of about 6 m s^{-1} d^{-1} in data composites of developing tropical depressions. EFC was close to zero in composites of tropical depressions that did not develop.

The results of Challa and Pfeffer (1990) showed that a variation of EFC of 6 m s^{-1} d^{-1} was large enough to have a significant impact on the intensification rate of a weak tropical disturbance in a three-dimensional model simulation. This provides some evidence that the threshold value of 10 m s^{-1} d^{-1} used in this study is a reasonable choice to identify periods of significant environmental interaction.

Cases in which the radial band–averaged EFC was >10 m s^{-1} d^{-1} were examined in detail. Typically, a maximum in EFC appeared at a radius between 1000 and 1500 km (as determined from EFC on the 100 km radial grid) and moved radially inward with time. This behavior is consistent with evolution of EFC in other studies (Molinari and Vollaro 1990; Davidson et al. 1990). The events lasted for 1–3 days as a storm moved towards a trough in the midlatitude westerlies or an upper-level cold low in low latitudes.

Six of the 32 storms did not have a period of enhanced EFC, 17 storms had 1 enhanced EFC event, 5 storms had 2 events, and 4 storms had 3 events for a total of 39 events. Given that 371 synoptic times were included and there were 39 events, a period of enhanced EFC occurred about every 5 days. All of the storms without a period of enhanced EFC remained at tropical storm strength for 3 days or less (Allison and Iris in 1989; and Diana, Edouard, Fran, and Hortense in 1990).

Table 4 summarizes the enhanced EFC events. The storm response was determined from the intensity change in the 1–2 d following the period of enhanced EFC. About half of the events were moderate and half were strong. The storm intensified after the period of enhanced EFC in only 13 of the 39 cases. In 15 cases, the storm intensity decreased as the vertical shear increased or the storm moved over cold water. In all of the cases with increased shear, the same synoptic feature that caused the enhanced EFC also caused the increased shear.

In 10 cases, the storm became extratropical shortly after the period of enhanced EFC. All of the extratropical cases were at high latitudes, and all but one of the associated EFC events were strong.

The above results suggest that enhanced EFC may be associated with tropical cyclone intensification, but other environmental factors must also be taken into account. To further illustrate the types of responses to the enhanced EFC events, examples from 1989 Hurricanes Dean and Gabrielle and 1990 Tropical Storm Arthur are presented.

Figure 2 shows the EFC as a function of radius and time for Hurricane Dean. The region of enhanced EFC first appeared on 4 August at a radius of 1500 km and moved inward during the next two days. This event began just as Dean was making a fairly sharp turn towards the north, as can be seen in Fig. 1a. The storm intensity was constant at 75 kt during the period of enhanced fluxes, but increased to 90 kt during the next 24 h. Figure 2 also shows that VSST was about 130 kt during the period of enhanced fluxes, indicating that there was potential for further intensification based upon SST. VSST began to decrease, beginning on 6 August as Dean moved toward colder water. It was

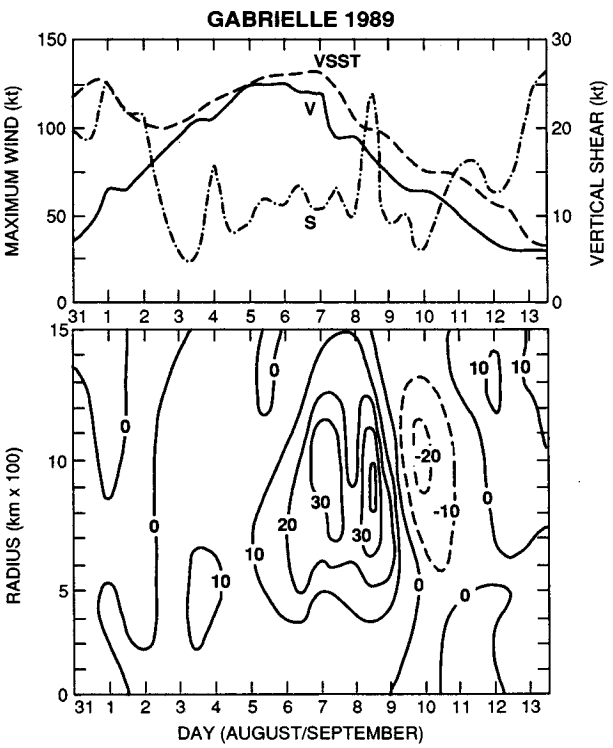

FIG. 4. Same as Fig. 2 but for Hurricane Gabrielle.

during this period that the intensification took place. For a short period beginning on 8 August, the observed maximum winds exceeded VSST as Dean moved over very cold water and was beginning to take on extratropical characteristics. Figure 2 also shows that the vertical shear decreased on 6 August at the end of the period of enhanced fluxes. This decreased shear may have also been a factor in the subsequent intensification of the storm.

Figure 3 shows the 200-mb wind field from the spline analysis at 1200 UTC 5 August, just before the time of maximum EFC. This figure shows that the enhanced EFC was due to the interaction of the storm with an elongated trough to the north and west of the storm center. This trough extended through a fairly deep layer and caused the turn towards the north seen in Fig. 1a.

Figure 2 illustrates the presence of a small region with EFC >10 m s^{-1} d^{-1} on 1 August, when the system was developing from an easterly wave. The enhanced EFC was due to an elongated trough at 200 mb to the north of the developing storm. This interaction was probably important for the initial formation of Dean.

Figure 4 shows the EFC as a function of radius and time for Hurricane Gabrielle. The period of enhanced EFC began on 5 September as the storm was making a gradual turn toward the north (Fig. 1a). The EFC reached a maximum on 7 September, decreased slightly, and reached a second maximum on 8 September. The second maximum, with a peak value of 48 m s^{-1} d^{-1}, was the largest of any storm in the 3-year sample.

Figure 5 shows the 200-mb wind field at 0000 UTC 8 September, just before the second maximum in EFC. The storm was interacting with a trough in the westerlies to the north of the storm center. This trough was moving rapidly toward the east, and the EFC decreased rapidly beginning on 9 September. There was also a secondary trough to the southwest of the storm center. The first maximum in EFC seen in Fig. 4 was associated with the trough to the southwest.

Figure 4 shows that, despite the large values of EFC, the storm was gradually decaying during the period after 5 September. However, the maximum winds of the storm were very close to VSST, indicating that there

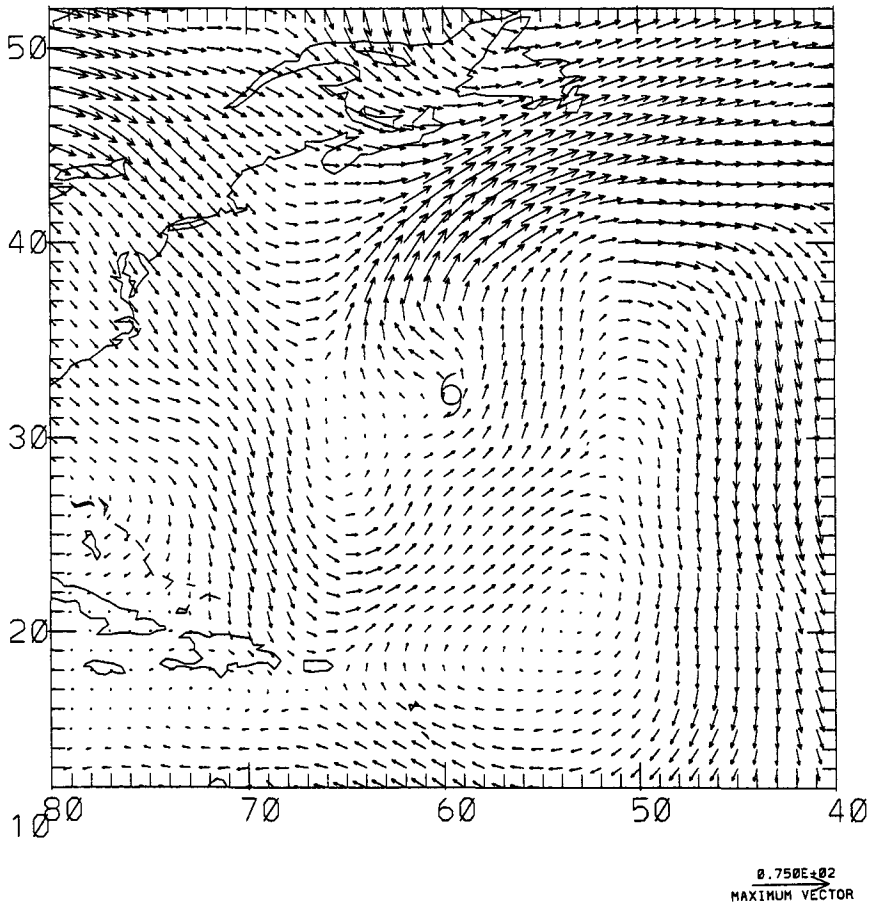

FIG. 5. Same as Fig. 3 but for Hurricane Gabrielle at 0000 UTC 0800 September 1989. Maximum wind vector: 75 m s^{-1}.

was not much potential for further development. The decrease in the maximum wind closely paralleled the decrease in VSST as the storm moved toward cold water. Figure 4 also shows that during the period of enhanced EFC, the vertical shear changed very little, except for a brief period on 8 September. Thus, even though the EFC and vertical shear were favorable for intensification, the storm intensity was limited by SST.

Figure 6 shows the EFC as a function of radius and time for Tropical Storm Arthur. The region of enhanced EFC began on 24 July as Arthur was developing from a tropical wave. Figure 7 shows the 200-mb wind field at 0000 UTC 26 July, at the time of the maximum EFC. There was a trough to the northeast of the storm center and a small cutoff cyclonic circulation (cold low) to the west of the storm center. As the storm moved toward the cold low (Fig. 1b) the vertical shear increased rapidly, beginning on 25 July. This increase in shear caused the storm to decay rapidly after 26 July, despite the enhanced EFC. The values of VSST in Fig. 6 were much larger than the observed maximum winds, indicating that SST did not limit the intensification.

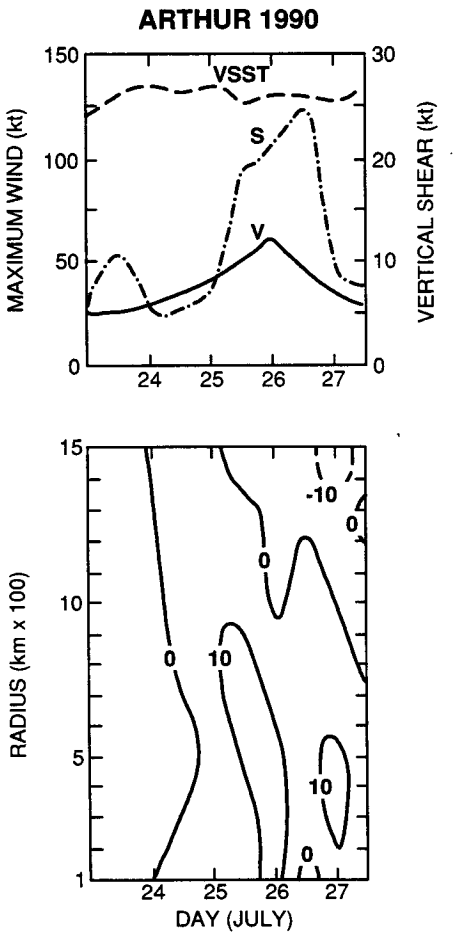

FIG. 6. Same as Fig. 2 but for Tropical Storm Arthur.

4. Regression analysis

To determine the statistical significance of the relationship between EFC and tropical cyclone intensity change, a regression analysis was performed. The EFC values in each of the radial bands were correlated with the intensity change of the storm in the following 12, 24, . . . , 72 h. All landfalling cases were eliminated, since the statistical properties of the intensity changes are quite different once a storm moves over land. The intensity changes for the periods after the storm became extratropical were also removed from the sample. After these modifications, there were 350 cases that had a 12-h intensity change and 206 cases with a 72-h change.

For comparison, the vertical shear (S) and a quantity P that takes into account SST effects were also correlated with intensity change. P is defined as

$$P = \text{VSST} - V, \tag{5}$$

where V is the intensity of the storm at the synoptic time. To include the time variations in SST, VSST in (5) was averaged along the storm track. For example, for the 12-h intensity change period, VSST in (5) is the average of VSST at the initial and 12-h positions of the storm.

Similar to VSST, the vertical shear used in the regression analysis was averaged along the track of the storm. However, all of the shear values in the average were obtained from the initial analysis. For this purpose, the azimuthally averaged radial and tangential winds at 850 and 200 mb were subtracted before the shear was calculated along the track of the storm. Since the synoptic flow evolves with time, only values out to 36 h were used in the average. Thus, the same value of S was used for the 36–72-h regressions for each synoptic time. The observed values of shear along the track could have been used in the average instead of the values estimated from the initial analyses. However, it is possible that the vertical shear in the vicinity of a storm decreases as it intensifies. If the observed shears were used, the distinction between cause and effect would be unclear.

Figure 8 shows the regression coefficients for P, S, and EFC. Each independent and dependent variable was normalized by subtracting the mean and dividing by the standard deviation. This normalization allows the comparison of the regression coefficients for different variables and different intensity change intervals (e.g., Steel and Torrie 1980). The confidence levels of the regression coefficients were determined using a standard F statistic. The variable $P(S)$ is positively (negatively) correlated with intensity change, and these relationships were statistically significant at the 95% level at all time periods between 12 and 72 h. Figure 8 also shows that EFC is negatively correlated with

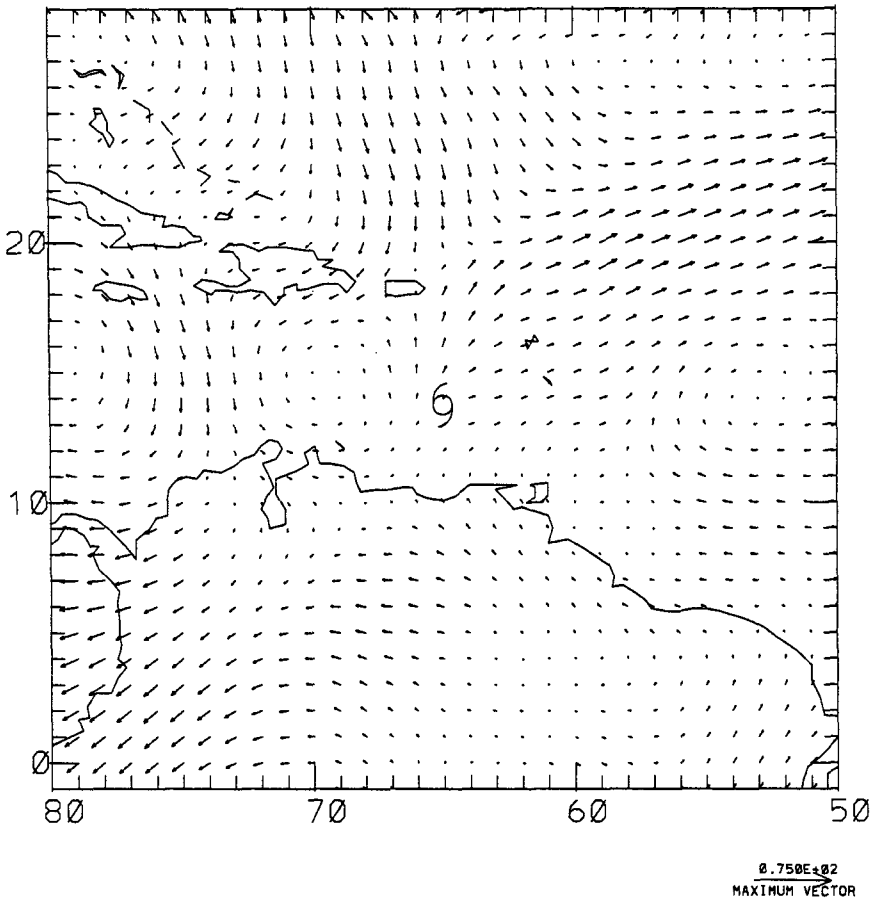

FIG. 7. Same as Fig. 3 but for Tropical Storm Arthur at 0000 UTC 26 July 1990. Maximum wind vector: 75 m s.

intensity change for nearly all of the radial bands, and the relationships were significant in some cases. The negative correlations between EFC and intensity change are not surprising in light of the results summarized in Table 4. In about two-thirds of the cases, the storm intensity decreased following periods of enhanced EFC due to increased vertical shear, decreasing SST, or because the storm became extratropical. Also, some of the largest values of EFC were associated with high-latitude storms.

The effects of SST and vertical shear could be removed by stratifying the sample by P and S. However, if even a small number (say about 5) of categories were chosen for each parameter, the sample size in each group would become fairly small. Another method that can account for the linear dependence of the intensity change on P and S is a multiple regression analysis using P, S, and EFC as independent variables. Figure 9 shows the regression coefficients from the multiple regressions. The coefficients for P and S at a given time interval were different for each radial band of EFC. However, the variation in the coefficients for P and S was very small, and the average coefficients are shown in Fig. 9. The relationships between P or S and intensity change were significant at the 95% level for every radial band.

Figure 9 shows that the regression coefficients for P and S in the multiple regressions are about the same as the coefficients for the individual regressions shown in Fig. 8. However, the coefficients for EFC were quite different in Fig. 9 than in Fig. 8. When the linear dependence on P and S is taken into account, EFC is positively correlated with intensity change. These correlations are statistically significant for the inner two radial bands for the 48-h intensity change interval.

The fact that the maximum correlation is for the 48-h time interval indicates that there is a time lag between the environmental interaction and the storm intensification. The observed time lag is consistent with the hypothesis that the intensification results from the effect of the EFC on the convection. If the convection is altered due to environmental interaction, it may take some time for the storm to reorganize. A lag between the environmental interaction and storm response was also noted by Molinari and Vollaro (1989), although the time lag in their study was somewhat shorter (about 30 h), and their correlation was with the momentum flux rather than the momentum flux convergence.

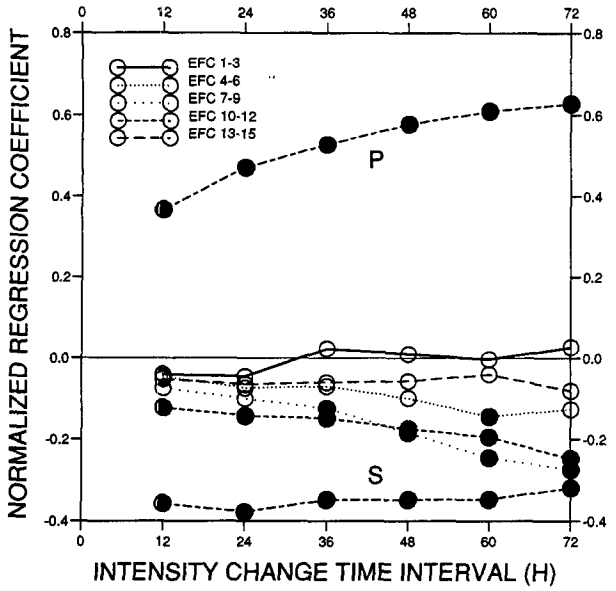

FIG. 8. Normalized regression coefficients for vertical shear (S), the sea surface temperature variable (P), and the eddy flux convergence (EFC) in each radial band (1–3 denotes the 100–300-km average). A separate regression was performed for each variable and for each intensity change time interval. The circles are filled for coefficients that were significant at the 95% level.

5. Environmental interactions for rapidly developing storms

Holland and Merrill (1984) speculated that although tropical cyclones can intensify without significant environmental interactions, extremely rapid intensification might require some interaction with upper-level systems. To investigate this possibility, the ten storms with the largest 48-h intensification rates were examined. The 48-h period was chosen since this interval had the strongest correlation with EFC in Fig. 9. The synoptic time at the beginning of the 48-h intensification period and the properties of each storm are listed in Table 5.

Table 5 shows that the periods of rapid intensification began before the storms reached hurricane intensity. All of the storms were in fairly low latitudes and over warm water (SST exceeded 27°C in all cases except Dean). The vertical shear was less than or equal to the total sample average in nine of the ten cases. The average EFC was greater than the sample average for the 100–300-km radial band, but less than average in the 400–700- and 800–1000-km bands. Examination of the EFC and the 200-mb analyses 24 h before and after the times listed in Table 5 showed that the intensification of Bob, Dean, and Klaus were associated with moderate EFC events and the intensification of Chantal was associated with a strong EFC event. The intensification of Gustav and Nana were also associated with the interaction with an upper-level trough, but the EFC values were not quite large enough to be classified as moderate events. Thus, six of the ten rapidly developing cases were associated with enhanced EFC due to the interaction with upper-level troughs.

As an example of an upper-level flow pattern with enhanced EFC, Fig. 10 shows the 200-mb wind for Bob at 0000 UTC 17 August 1991. The intensity of Bob increased by 55 kt in the next 48 h. Bob interacted with the upper-level cold low located to the southeast of the storm. After this time Bob moved toward the north, away from the cold low. The 200-mb winds for Bob were similar to the other rapidly developing cases with enhanced EFC in that the storm was located on the edge of an upper-level cyclonic feature. However, the other rapidly developing storms with enhanced EFC were located south or east of a trough in the westerlies, rather than north of a cold low.

Figure 11 shows the 200-mb flow for Hugo at 1200 UTC 13 September 1989. The intensity of Hugo increased by 65 kt in the next 48 h. Hugo was located on the south side of an anticyclone. However, there were no apparent cyclonic disturbances near the storm to enhance the EFC.

The above results suggest that the interaction with upper-level troughs can lead to rapid intensification. However, rapid intensification may also be possible when an organized tropical cyclone is over warm water in a low shear environment but without interaction with upper-level troughs.

6. Concluding remarks

The eddy flux convergence of relative angular momentum (EFC) at 200 mb was calculated for the named tropical cyclones during the 1989–1991 Atlantic

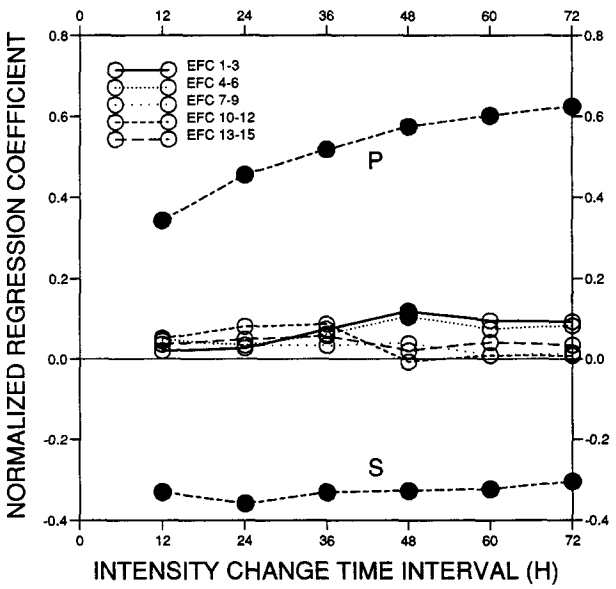

FIG. 9. Same as Fig. 8, but for multiple regressions that included three independent variables (EFC in a given radial band, P, and S) for each intensity change time interval.

TABLE 5. Characteristics of rapidly intensifying storms.

Storm	Date (mo/d/yr)	Time (h UTC)	Lat. (°N)	48-h Intensity change (kt)	Initial intensity (kt)	SST (°C)	SHR (kt)	EFC ($m\ s^{-1}\ d^{-1}$) 1–3	4–6	7–9
Claudette	9/05/91	12	26.2	80	35	28.0	2	−1	−2	−3
Hugo	9/13/89	12	12.8	65	60	27.1	9	2	2	2
Bob	8/17/91	00	27.1	55	40	28.6	6	1	1	5
Chantal	7/30/89	12	22.5	50	20	28.6	10	5	19	23
Isidore	9/05/90	12	10.0	50	35	27.4	8	3	3	1
Gustav	8/25/90	12	13.7	45	35	27.5	6	3	5	1
Nana	10/16/90	12	22.3	45	30	27.9	11	3	−6	−12
Gabrielle	8/31/89	12	11.5	40	45	27.5	16	−1	−3	−4
Dean	8/01/89	12	15.4	40	30	26.0	15	2	7	6
Klaus	10/03/90	12	15.6	40	30	28.4	25	5	4	5
Ten-case average			17.7	51	36	27.7	11	2	3	2
Total sample average			22.9	6	56	26.8	16	1	4	5

hurricane seasons (371 synoptic times). A period of enhanced EFC within 1500 km of the storm center occurred about every 5 days due to the interaction with upper-level troughs in the midlatitude westerlies or upper-level cold lows in low latitudes. Twenty-six of the 32 storms had at least one period of enhanced EFC.

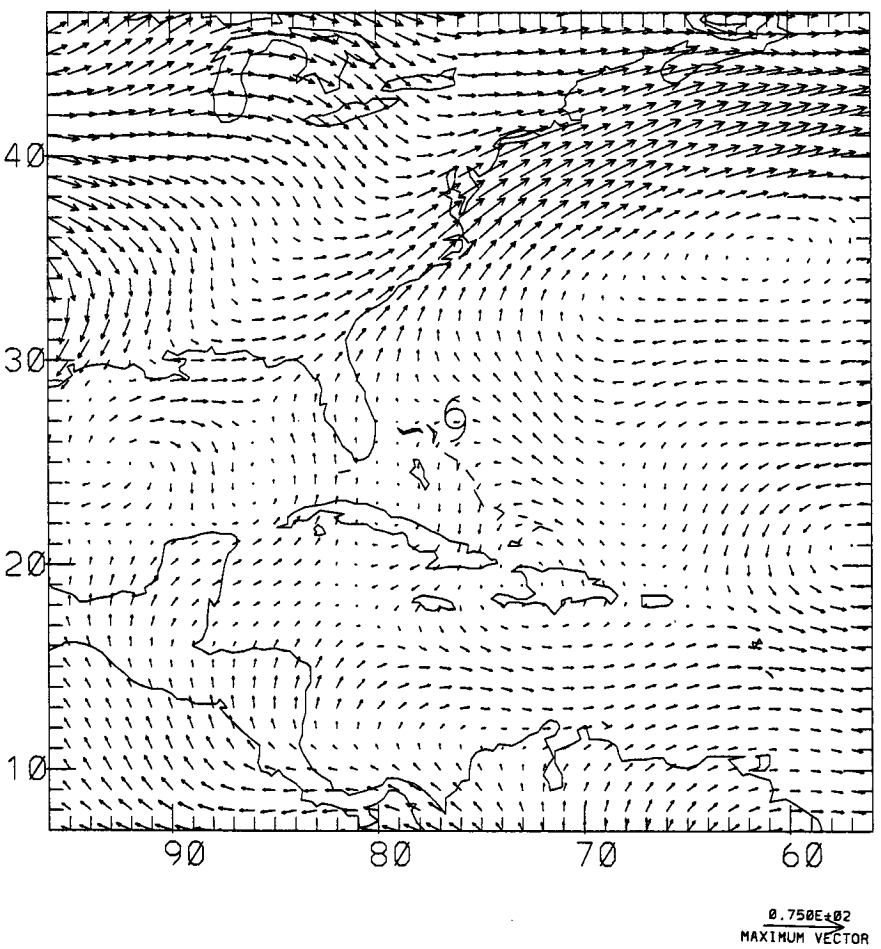

FIG. 10. Same as Fig. 3 but for Hurricane Bob at 0000 UTC 17 August 1991.

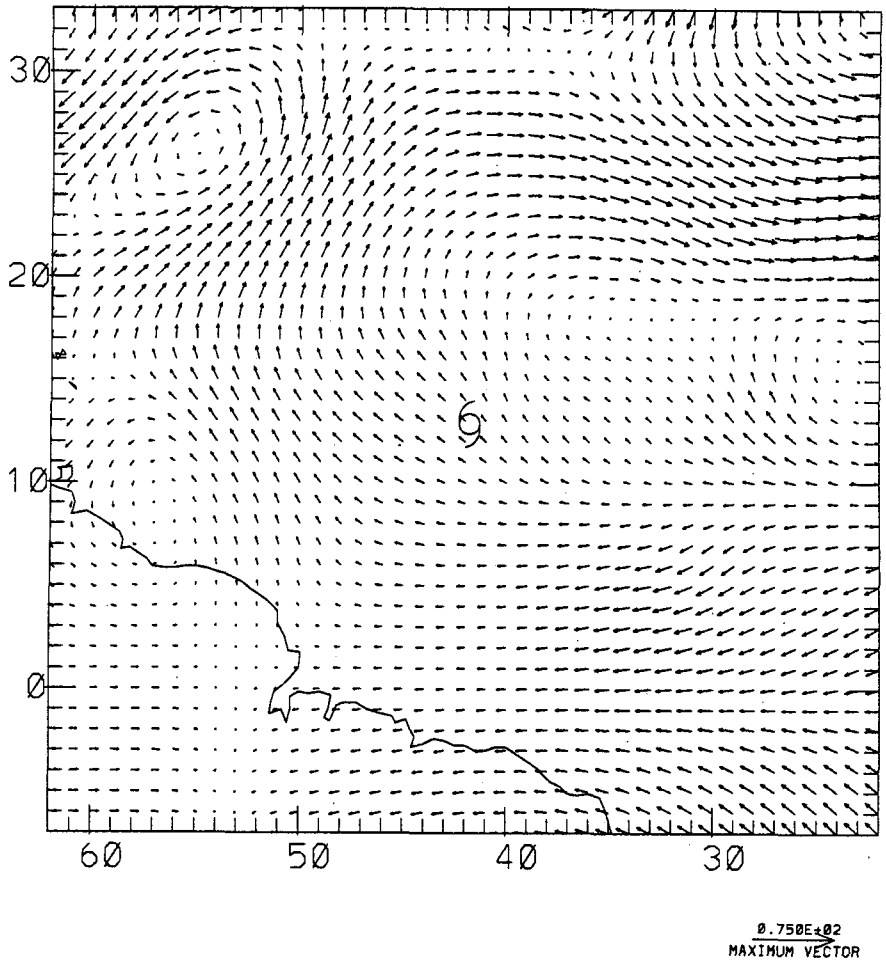

FIG. 11. Same as Fig. 3 but for Hurricane Hugo at 1200 UTC 13 August 1989.

In about one-third of the cases, the storm intensified just after the period of enhanced EFC. In most of the cases where the storm did not intensify, the vertical shear increased, the storm moved over cold water, or the storm became extratropical just after the period of enhanced EFC. A statistically significant relationship (at the 95% level) was found between the EFC within 600 km of the storm center and the intensity change during the next 48 h. However, this relationship could only be determined using a multiple regression technique that also accounted for the effects of vertical shear and sea surface temperature variations.

The EFC was also examined for the ten storms from the 1989–1991 sample that had the largest intensification rates. Six of the 10 periods of rapid intensification were associated with enhanced EFC. In the remaining four cases, the storms were intensifying rapidly in a low shear environment without any obvious interaction with upper-level troughs.

The results from this study indicate that environmental influences on tropical cyclone intensity change can be positive or negative. The vertical shear has a strong negative influence on intensification and was highly correlated with weakening in the statistical analysis. In the rapidly intensifying cases, the EFC was enhanced in six of the ten cases, but the vertical shear remained low. The 200-mb analyses showed that for these cases, the storms were on the edge of upper-level cyclonic features, but never moved directly under them. Thus, the orientation of the upper-level cyclonic features relative to the storm is a critical factor for determining whether the environmental interactions will be positive or negative.

The multiple regressions using vertical shear, the sea surface temperature parameter, and EFC as independent variables explained about 50% of the variance in the intensity changes at 36–72 h. These independent variables are being combined with climatological variables to develop a statistical hurricane intensity prediction scheme for Atlantic tropical cyclones (DeMaria and Kaplan 1991).

In this study, the eddy fluxes of heat were neglected. The effects of eddy heat and momentum fluxes can be combined by casting the problem in terms of potential

vorticity. The basic idea is that within the confines of a suitable balance approximation, the three-dimensional mass and wind fields can be recovered from the potential vorticity (Hoskins et al. 1985). The interaction between a tropical cyclone and a synoptic-scale weather system could then be viewed as the response that occurs when two regions of potential vorticity are brought together by the vertical shear in the flow. The difficulty with this approach, however, is the determination of a balance approximation that is valid for the tropical cyclone and the large-scale flow. The classical quasigeostrophic equations or the semigeostrophic equations described by Hoskins (1975) are not valid in the vicinity of highly curved flows. The balanced vortex model of Eliassen (1952) includes the effects of curvature but requires the assumption of axial symmetry, and so is not valid in the storm environment.

The eddy momentum fluxes were calculated only at 200 mb in this study. Detailed observations of the three-dimensional structure of the hurricane outflow layer are extremely scarce, primarily because of the altitude limitations of the NOAA WP-3D and U.S. Air Force reconnaissance aircraft. During the recent TCM-90 experiment (Elsberry and Abbey 1991), dropsonde observations were obtained from 200 mb to the surface in the vicinity of four typhoons in the western Pacific, using the NASA DC-8. This dataset may prove to be very useful in the study of the interaction of tropical cyclones with synoptic-scale weather systems.

Acknowledgments. Part of this research was done while the second author was a visiting scientist at AOML. Support from the Cooperative Institute for Marine and Atmospheric Science (CIMAS) of the University of Miami is acknowledged. The authors would like to thank John Molinari, Greg Holland, Vic Ooyama, and Hugh Willoughby for their comments on this work.

REFERENCES

Anthes, R. A., 1982: *Tropical Cyclones: Their Evolution, Structure and Effects. Meteor. Monogr.*, No. 41, Amer. Meteor. Soc., 208 pp.

Challa, M., and R. L. Pfeffer, 1990: Formation of Atlantic hurricanes from cloud clusters and depressions. *J. Atmos. Sci.*, **47**, 909–927.

Davidson, N. E., G. J. Holland, J. L. McBride, and T. D. Keenan, 1990: On the formation of AMEX tropical cyclones Irma and Jason. *Mon. Wea. Rev.*, **118**, 1981–2000.

DeMaria, M., and J. Kaplan, 1991: A statistical model for predicting tropical cyclone intensity change. Preprints, *19th Conf. on Hurricanes and Tropical Meteorology*, Miami, Amer. Meteor. Soc., 521–526.

——, S. D. Aberson, K. V. Ooyama, and S. J. Lord, 1992: A nested spectral model for hurricane track forecasting. *Mon. Wea. Rev.*, **120**, 1628–1643.

Eliassen, A., 1952: Slow thermally or frictionally controlled meridional circulation in a circular vortex. *Astrophys. Norv.*, **5**, 19–60.

Elsberry, R. L., and R. F. Abbey Jr., 1991: Overview of the tropical cyclone motion (TCM-90) field experiment. Preprints, *19th Conf. Hurricanes and Tropical Meteorology*, Miami, Amer. Meteor. Soc., 1–6.

Emanuel, K. A., 1988: The maximum intensity of hurricanes. *J. Atmos. Sci.*, **45**, 1143–1155.

Gray, W. M., 1968: Global view of the origin of tropical disturbances and storms. *Mon. Wea. Rev.*, **96**, 669–700.

Holland, G. J., and R. T. Merrill, 1984: On the dynamics of tropical cyclone structure changes. *Quart. J. Roy. Meteor. Soc.*, **110**, 723–745.

Hoskins, B. J., 1975: The geostrophic momentum approximation and the semigeostrophic equations. *J. Atmos. Sci.*, **32**, 233–242.

——, M. E. McIntyre, and A. W. Robertson, 1985: On the use and significance of isentropic potential vorticity maps. *Quart. J. Roy. Meteor. Soc.*, **111**, 877–946.

Jarvinen, B. R., C. J. Neumann, and M. A. S. Davis, 1984: A tropical cyclone data tape for the North Atlantic basin, 1885–1983: Contents, limitations, and uses. NOAA Tech. Memo. NWS, NHC-22, 21 pp. [Available from NWS/National Hurricane Center, Coral Gables, FL 33146.]

Khain, A., and I. Ginis, 1991: The mutual response of a moving tropical cyclone and the ocean. *Contrib. Atmos. Phys.*, **64**, 125–142.

Levitus, S., 1982: *Climatological Atlas of the World Ocean.* NOAA Prof. Paper 13, U.S. Govt. Printing Office, Washington, D.C., 20402.

Lord, S. J., and J. L. Franklin, 1987: The environment of Hurricane Debby. Part I: Winds. *Mon. Wea. Rev.*, **115**, 2760–2780.

McBride, J. L., 1981: Observational analysis of tropical cyclone formation. Part III: Budget analysis. *J. Atmos. Sci.*, **38**, 1152–1166.

Merrill, R. T., 1988: Environmental influences on hurricane intensification. *J. Atmos. Sci.*, **45**, 1678–1687.

Molinari, J., and D. Vollaro, 1989: External influences on hurricane intensity. Part I: Outflow layer eddy-angular momentum fluxes. *J. Atmos. Sci.*, **46**, 1093–1105.

——, and ——, 1990: External influences on hurricane intensity. Part II: Vertical structure and response of the hurricane vortex. *J. Atmos. Sci.*, **47**, 1902–1918.

——, ——, and F. Robasky, 1992: Use of ECMWF operational analyses for studies of the tropical cyclone environment. *Meteor. Atmos. Phys.*, **47**, 127–144.

Montgomery, M. T., and B. F. Farrell, 1993: Tropical cyclone formation. *J. Atmos. Sci.*, **50**, 285–310.

Ooyama, K. V., 1987: Scale-controlled objective analysis. *Mon. Wea. Rev.*, **115**, 2479–2506.

Pfeffer, R. L., 1958: Concerning the mechanism of hurricanes. *J. Meteor.*, **15**, 113–120.

——, and M. Challa, 1981: A numerical study of the role of eddy fluxes of momentum in the development of Atlantic hurricanes. *J. Atmos. Sci.*, **38**, 2393–2398.

——, and ——, 1991: Formation of Atlantic hurricanes from cloud clusters and depressions. Preprints, *19th Conf. on Hurricanes and Tropical Meteorology*, Miami, Amer. Meteor. Soc., 214–216.

Sadler, J. C., 1976: A role of the tropical upper-tropospheric trough in early-season typhoon development. *Mon. Wea. Rev.*, **104**, 1266–1278.

Steel, R. G. D., and J. H. Torrie, 1980: *Principles and Procedures of Statistics: A Biometrical Approach.* (2d ed.) McGraw-Hill, [ISBN 0-07-060926-8.] 633 pp.